

✓ 28p S 54331 R 30

NASA TM X-36

~~N62-71860~~N63-12977  
code-1

# TECHNICAL MEMORANDUM

## X - 36

FLIGHT INVESTIGATION OF THE EFFECT OF  
DISTRIBUTED ROUGHNESS ON SKIN DRAG OF

A FULL-SCALE AIRPLANE

By Edwin J. Saltzman

High-Speed Flight Station  
Edwards, Calif.

Declassified December 18, 1961

NATIONAL AERONAUTICS AND SPACE ADMINISTRATION  
WASHINGTON

September 1959

## NATIONAL AERONAUTICS AND SPACE ADMINISTRATION

## TECHNICAL MEMORANDUM X-36

## FLIGHT INVESTIGATION OF THE EFFECT OF

## DISTRIBUTED ROUGHNESS ON SKIN DRAG OF

## A FULL-SCALE AIRPLANE

By Edwin J. Saltzman

## SUMMARY

The change in drag caused by the addition of two sizes of distributed sand-type roughness to the wings and tail surfaces of a delta-wing airplane has been measured at Mach numbers near 0.8 and 1.1.

The largest roughness, 0.006-inch mean effective diameter, caused an increase of about 0.0030 in overall airplane drag coefficient at a Mach number of 0.8 and about 0.0023 at a Mach number of 1.1. These values represent an increase in drag force of about 1,000 pounds at free-stream Reynolds numbers of the order of 45 to 60 million for dynamic pressures between 550 and 650 pounds per square foot, which is equal to about 1 pound of added drag for each square foot of roughened area. Calculated skin drag coefficients based upon the increase in drag caused by the largest roughness agree reasonably well with the increase predicted by the low-speed drag law for a rough plate for turbulent-flow conditions.

The increase in drag caused by the addition of the smallest roughness, 0.002-inch mean effective diameter, was less than half the increase predicted by the low-speed drag law for a rough plate. This indicates that, for turbulent-flow conditions and chord Reynolds numbers of the order of 50 to 60 million, surfaces can be much rougher than conventional painted surfaces or conventional alloy sheet metal without causing a significant increase in airplane drag.

## INTRODUCTION

Recently, great emphasis has been placed on research in the field of boundary layer, especially the skin-friction and heat-transfer aspects

of the subject. In response to requests for full-scale flight skin-friction and boundary-layer transition data, the NASA High-Speed Flight Station at Edwards, Calif. has conducted two concurrent studies of a preliminary nature. One study investigates the extent of laminar run which can be achieved over a carefully maintained polished wing and a wing with a practical surface finish at Mach numbers up to approximately 2.0 (ref. 1). The second study, which is the subject of this paper, presents the change in drag on a delta-wing interceptor airplane caused by the addition of distributed sand-type roughness. An attempt is made to extract the net drag due to the roughness and to calculate a skin drag coefficient for the roughened surface.

Drag data are presented for three surface-roughness conditions at Mach numbers near 0.8 and 1.1. The altitude range was varied to provide an overall range in free-stream Reynolds number from about 2 million per foot to over 4 million per foot. Full-scale flight results are compared with wind-tunnel data and with the low-speed drag law for a rough plate in turbulent flow.

#### SYMBOLS

$A$	test-surface area or roughened area, $A_v + A_w$ , sq ft
$A_v$	test-surface area of vertical tail, 157 sq ft
$A_w$	test-surface area of wings, 1,023 sq ft
$a_l$	longitudinal acceleration, g units
$a_n$	normal acceleration, g units
$C_D$	drag coefficient, $D/qS$
$C_f$	skin drag coefficient, $D_s/qA$
$\Delta C_f$	increase in skin drag coefficient due to roughness for turbulent flow, $C_{f_{\text{rough}}} - C_{f_{\text{smooth}}}$
$C_L$	lift coefficient, $L/qS$
$D$	drag force along flight path, lb

$D_s$	skin drag force along flight path for the test surface, lb
$F_j$	jet thrust, lb
$F_r$	ram drag, lb
$g$	gravitational acceleration, ft/sec <sup>2</sup>
$h_p$	pressure altitude, ft
$k$	mean effective roughness diameter or height, in.
$L$	lift force normal to flight path, lb
$l$	mean test chord length, $\frac{l_v A_v + l_w A_w}{A_v + A_w}$ , 14.1 ft
$l_v$	mean chord of test surface, vertical tail, $\frac{\text{Length of inboard chord} + \text{Length of outboard chord}}{2}$ , 9.7 ft
$l_w$	mean chord of test surface, wings, $\frac{\text{Length of inboard chord} + \text{Length of outboard chord}}{2}$ , 14.8 ft
$M$	Mach number
$p_0$	free-stream static pressure, lb/sq ft
$q$	dynamic pressure, $0.7M^2 p_0$ , lb/sq ft
$R$	free-stream Reynolds number, $\frac{\rho V l}{\mu}$
$R_{ft}$	free-stream Reynolds number per ft
$S$	wing area, sq ft
$V$	true airspeed, ft/sec
$W$	airplane weight, lb
$\alpha$	angle of attack, deg



$\mu$  absolute viscosity, lb-sec/sq ft

$\rho$  air density, slugs/cu ft

Subscript:

min minimum

## AIRPLANE

The airplane used in the subject tests is a  $60^\circ$  delta-wing interceptor powered by a single turbojet engine with afterburner. The airplane does not have a horizontal tail, but utilizes elevons at the wing trailing edges for longitudinal control.

Detailed physical characteristics of the airplane are presented in table I. Photographs are shown in figure 1 and a three-view drawing in figure 2.

## INSTRUMENTATION

The airplane carried standard NASA instruments for measuring quantities pertinent to the determination of lift and drag.

Free-stream total and static pressures were obtained from locations 79 inches and 71 inches, respectively, ahead of the intersection of the airplane nose and the nose boom. Angle of attack was measured by a vane located 52 inches forward of this intersection.

Total temperature, used to calculate true airspeed, was measured by a shielded resistance-type probe located beneath the fuselage. Total and static pressure at the compressor face, used in calculating ram drag, were obtained by 30 probes (5 probes on each of 6 radial rakes) located immediately ahead of the compressor face, together with six flush static orifices located at the total-pressure survey stations. Tailpipe exit total pressure was obtained by an air-cooled probe located near the nozzle exit plane of the afterburner.

## ACCURACY

Calculations to determine the theoretical upwash at the angle-of-attack-vane location indicate a maximum value for upwash of about  $0.16^\circ$

at  $M \approx 0.8$  at an altitude of 40,000 feet (a more adverse condition than any included in the subject tests). Adjustments were not made to the data to account for these small values of upwash. For supersonic speeds, of course, upwash is theoretically zero. The effects of inertia loads upon the boom and on pitching velocity have been accounted for. Based upon these conditions, and special tests which were performed on a similar airplane-angle-of-attack system (ref. 2), it is believed that angle of attack is accurate to within  $\pm 0.25^\circ$  for lift coefficients up to 0.2.

The remaining instrumentation and techniques are similar to those used in reference 2, except that, for the present tests, the linear accelerometer data are adjusted for the effects of pitching velocity and pitching acceleration caused by displacement of the accelerometers from the airplane center of gravity.

On the basis of the experience related in reference 2 and the added refinements noted, it is concluded that the repeatability of unfaired data is within  $\pm 0.0005$  at  $C_{D_{min}}$  for a specific Mach number-altitude combination. Examination of the basic data indicates that values of  $C_{D_{min}}$  based upon fairings are consistent to within  $\pm 0.0003$  for a properly executed maneuver. Hence, the maximum error in calculated  $C_f$  is within  $\pm 0.0002$ , and these limits may be reduced somewhat where repeated test runs are made at specific test conditions (the number of test runs for each test condition is shown in table II). These favorable error limits account for calculated coefficients which are consistent within themselves and which are considered reliable. When comparing these data with theory, however, a possible limitation is the accuracy of the value  $k$ , effective roughness height. It is not known to what extent this limitation affects the comparisons shown.

## PROCEDURES

### Method of Calculating Thrust and Drag

The accelerometer method was used to determine lift and drag. This method employs the following equations, which are applicable if the thrust axis is parallel to the airplane longitudinal axis:

$$C_L = \left( \frac{W a_n}{qS} \right) \cos \alpha - \left( \frac{F_J - W a_l}{qS} \right) \sin \alpha$$

$$C_D = \left( \frac{F_J - W a_l}{qS} \right) \cos \alpha - \left( \frac{F_R}{qS} \right) + \left( \frac{W a_n}{qS} \right) \sin \alpha$$

The single-probe method was used to obtain tailpipe total pressure, used in computing  $F_j$ , and the inlet-duct method was employed in determining  $F_T$ . Details regarding these methods of measuring drag and thrust are available in reference 3.

### Flight-Test Conditions

The effects of the distributed roughness were studied at Mach numbers of about 0.8 and 1.1, inasmuch as at these values the change in air-plane drag coefficient with Mach number is essentially zero at the lift conditions of the tests. The altitude range for both the subsonic and supersonic tests was varied to provide a nominal variation in Reynolds number. (Henceforth, in this report any mention of Reynolds number will refer to free-stream values.) The Reynolds number ranged between about 2 million per foot to a little above 4 million per foot for both subsonic and supersonic tests. Reynolds number for the test surfaces reached values of about 60.6 million, based on the mean test chord length  $l$  of 14.1 feet. This length was considered to be more applicable than the mean aerodynamic chord to an analysis of skin drag.

The test maneuvers consisted of a push-down to near-zero lift, followed by a recovery. These maneuvers were made as nearly symmetrical with respect to the X-Z plane as possible and were executed as smoothly and uniformly as possible. Records were taken continuously throughout the maneuver to detect effects which might indicate a changing drag contribution of the longitudinal control surfaces. It was found that the drag-coefficient values for decreasing and increasing control deflection, or angle of attack, were indistinguishable; hence the effect of longitudinal control upon repeatability was negligible for a given lift condition. Center of gravity was maintained within the limits of 28 and 29 percent of the mean aerodynamic chord for all test maneuvers.

### Surface-Roughness Details

The basic surface conditions tested are given in the following table:

Configuration	Production finish (painted, but not polished)	Water paint impregnated with 220 grit	Water paint impregnated with 80 grit
Roughness or mean particle diameter	Root mean square reading 5 to 50 microinches	0.0025 in. (approx.)	0.0075 in. (approx.)
Mean effective particle diameter, $k$		0.002 in. (approx.)	0.006 in. (approx.)

According to reference 4, the mean effective diameter of a sand particle when bound to the test surface by paint is between 0.75 and 0.80 of the actual mean diameter.

The distributed sand-type roughness was placed on the upper and lower surfaces of both wings and on both sides of the vertical tail. This provided a roughened skin area (test surface) of about 1,180 square feet, which constituted about 54 percent of the total airplane skin area.

The 220-grit roughness was distributed on the test surface by mixing the grit with water paint and spraying with a conventional spray gun. The grit and paint were constantly agitated within the paint container by a motor-driven paddle. Typical distribution of this roughness is shown in figure 3.

The 80 grit was too coarse to spray through the available spray guns, so water paint was sprayed over an area of approximately 6 square feet, and a sandblast gun loaded with the 80 grit was used to apply a layer of grit onto the wet paint. This method was repeated until the entire test area was covered. This technique provided a roughness of acceptable uniformity (see fig. 4).

To ascertain if the production finish was experiencing a fully turbulent boundary layer, a transition strip composed of 80 grit distributed in a band 1 inch wide (fig. 5) was placed near the leading edge of all the test surfaces. The choice of 80 grit was based on unpublished flight results obtained at the High-Speed Flight Station and on the findings of reference 5. The remaining area of the test surfaces was in the production-finish condition (fig. 6). Several maneuvers were flown under these conditions, and the drag coefficients were compared with those for the production finish with natural transition. As is shown in the following section, these preliminary tests have established that the production-finish surface experienced turbulent flow over essentially the entire area for the natural-transition condition for Reynolds numbers down to the test limits of 3.2 million per foot for the subsonic tests and 3.7 million per foot for the supersonic tests. Hence, for this Reynolds number range each of the three test surfaces (see preceding table) experiences turbulent flow. Figure 7 gives a summary of the flight conditions for the various test surfaces.

## RESULTS

### Overall Drag Measurements

Presentation. - Overall drag coefficient as a function of lift for each test condition is presented in figures 8 to 11. The drag coefficient

$C_D$  is based on a total wing area of 695 square feet, which includes the projected area within the fuselage. Figure 8 presents these data for the production finish with natural transition. The measured minimum drag coefficient is reduced significantly by decreasing Reynolds number (increasing altitude) for the supersonic tests. The possible increase of skin area experiencing laminar flow at reduced Reynolds numbers can account for only a part of this decrease in drag. It is believed that much of this apparent drag-coefficient reduction is caused by variations in base drag and calculated jet thrust, which are affected by altitude and have not been accounted for. This, however, does not affect the conclusions of this paper, which are based upon drag increments for different roughness values at a fixed altitude and proved turbulent-flow conditions.

Butt joints and protruding rivet heads near the leading edges should insure turbulent-flow conditions for the production finish at the highest Reynolds numbers. However, it was considered desirable to verify this belief by measuring the overall drag under known turbulent conditions. For this reason a comparison was made (fig. 9) between drag for the production finish with natural and forced transition. (See preceding section for description of tripping device.) As would be expected, figure 9 shows that within the accuracy of the measurements the production finish with natural transition experiences turbulent flow over essentially the entire test area at Reynolds numbers down to the test limits of 3.2 million per foot for the subsonic tests and 3.7 million per foot for the supersonic tests.

Figures 10 and 11 show overall drag coefficient as a function of lift for the wing and tail surfaces covered with 220 grit and 80 grit, respectively. Figure 12 presents selected examples of overall drag coefficient for all of the test surfaces. All of the basic data presented thus far are summarized briefly in table II in which the mean values of drag coefficient near minimum drag are compared for the various surface conditions.

Discussion.- As can be seen in table II, the increase in drag coefficient caused by the addition of the 220-grit roughness is of the order of 0.0005 at the two highest test Reynolds numbers where turbulent flow is known to exist. The drag-force increase is about 200 pounds at these Reynolds numbers, or about 0.2 pound per square foot of roughened area.

At the lower Reynolds numbers, 3.2 million per foot and below, there is, seemingly, an increase in drag coefficient of about 0.0012 caused by the 220-grit roughness. These results are inconclusive, however, because it cannot be ascertained that the production-finish data represent turbulent flow. In fact, it is rather obvious that appreciable laminar flow was experienced at these conditions. A mean length of laminar run of the order of 1.5 to 2 feet on the production finish would account for the disagreement between the results of the two highest test Reynolds numbers and the two lower Reynolds numbers.

The drag-coefficient increase caused by the addition of the 80-grit roughness is much more significant, amounting to about 0.0030 for the subsonic tests and about 0.0023 at  $M \approx 1.1$ . Interpreted in terms of drag force, this increase amounts to about 1,000 pounds for dynamic-pressure values between 550 and 650 pounds per square foot, or approximately 1 pound of added drag for each square foot of roughened area.

### Skin Drag Coefficient

H  
1  
1  
2  
If it is assumed that the skin friction of the test surface for the production finish is equal to the friction drag of a smooth flat plate for equivalent area and flow conditions, the increment of drag increase due to the roughness can be used to calculate the effective skin drag coefficient of the roughened surface. This calculation has been made by using the theoretical curves obtained by the extended Frankl-Voishel method (ref. 6) to estimate the turbulent-flow skin-friction coefficient for the production finish at the test conditions. The resulting calculated skin drag coefficients are shown in table III, in which they are compared with terminal skin drag coefficients obtained from expressions given in references 7 and 8. (Terminal skin drag coefficient is reached for turbulent flow on rough surfaces when the coefficient remains constant with increasing Reynolds number, varying only with roughness height.) Table III indicates that terminal values of skin drag coefficient were approached for the 80-grit roughness, but that for the 220-grit finish the values are only about 10 to 15 percent higher than what would be expected for a smooth surface, production finish.

A comparison of the measured increase in skin drag coefficient caused by roughness with the increase predicted by the low-speed drag law for a rough plate (ref. 7) is shown in figure 13. The 80-grit ( $k/l \approx 3.4 \times 10^{-5}$ ) results for  $M \approx 0.8$  approach the values predicted for a similar roughness height-chord length ratio; however, the measured results for  $M \approx 1.1$  fall significantly lower than the values for  $M \approx 0.8$ . This trend of decreasing skin drag coefficient with increasing Mach number agrees with the findings of reference 9 and the theoretical methods discussed in reference 6; however, the magnitude of the skin drag-coefficient decrease for the present tests is greater than is indicated by these references.

The measured skin drag-coefficient increase caused by the addition of the 220 grit ( $k/l \approx 1.1 \times 10^{-5}$ , fig. 13) is less than half the increase predicted by the low-speed drag law for a rough plate under turbulent-flow conditions. It is important to realize that the 220-grit finish is much rougher than a conventional painted surface, even much rougher than camouflage paint. Therefore, the present results indicate that for chord Reynolds numbers of the order of 50 to 60 million, surfaces for turbulent-flow conditions can be much rougher than conventional painted surfaces or conventional alloy sheet metal without causing a significant increase in airplane drag.

## CONCLUSIONS

The addition of two sizes of distributed sand-type roughness to the wings and tail surfaces of a delta-wing airplane provided the following results:

1. The largest roughness, 0.006-inch mean effective diameter, caused an increase of about 0.0030 in overall airplane drag coefficient at a Mach number of 0.8 and about 0.0023 at a Mach number of 1.1. These values represent an increase in drag force of about 1,000 pounds at free-stream Reynolds numbers of the order of 45 to 60 million for dynamic pressures between 550 and 650 pounds per square foot, which is equal to about 1 pound of added drag for each square foot of roughened area.

2. The increase in drag caused by the largest roughness resulted in calculated skin drag coefficients which agree reasonably well with the increase predicted by the low-speed drag law for a rough plate for turbulent-flow conditions.

3. The increase in drag caused by the addition of the smallest roughness, 0.002-inch mean effective diameter, was less than half the increase predicted by the low-speed drag law for a rough plate. This indicates that for turbulent-flow conditions and for chord Reynolds numbers of the order of 50 to 60 million, surfaces can be much rougher than conventional painted surfaces or conventional alloy sheet metal without causing a significant increase in airplane drag.

High-Speed Flight Station,  
National Aeronautics and Space Administration,  
Edwards, Calif., March 17, 1959.

## REFERENCES

1. Banner, Richard D., McTigue, John G., and Petty, Gilbert, Jr.: Boundary-Layer-Transition Measurements in Full-Scale Flight. NACA RM H58E28, 1958.
2. Saltzman, Edwin J., Bellman, Donald R., and Musialowski, Norman T.: Flight-Determined Transonic Lift and Drag Characteristics of the YF-102 Airplane With Two Wing Configurations. NACA RM H56E08, 1956.
3. Beeler, De E., Bellman, Donald R., and Saltzman, Edwin J.: Flight Techniques for Determining Airplane Drag at High Mach Numbers. NACA TN 3821, 1956.
4. Hoerner, Sigward F.: Fluid-Dynamic Drag. Pub. by the author (148 Busteed, Midland Park, N. J.), 1958.
5. von Doenhoff, Albert E., and Horton, Elmer A.: A Low-Speed Experimental Investigation of the Effect of a Sandpaper Type of Roughness on Boundary-Layer Transition. NACA TN 3858, 1956.
6. Rubesin, Morris W., Maydew, Randall C., and Varga, Steven A.: An Analytical and Experimental Investigation of the Skin Friction of the Turbulent Boundary Layer on a Flat Plate at Supersonic Speeds. NACA TN 2305, 1951.
7. Schlichting, Hermann: Lecture Series "Boundary Layer Theory." Part II - Turbulent Flows. NACA TM 1218, 1949.
8. Droblenkov, V. F.: The Turbulent Boundary Layer on a Rough Curvilinear Surface. NACA TM 1440, 1958.
9. Sevier, John R., Jr., and Czarnecki, Kazimierz R.: Investigation of Effects of Distributed Surface Roughness on a Turbulent Boundary Layer Over a Body of Revolution at a Mach Number of 2.01. NACA TN 4183, 1958.



TABLE I.- TABLE OF PHYSICAL CHARACTERISTICS

## Wing:

Airfoil section . . . . .	NACA 0004-65 (Modified)
Total area, sq ft . . . . .	695.05
Span (actual), ft . . . . .	38.17
Mean aerodynamic chord, ft . . . . .	23.76
Root chord, ft . . . . .	35.63
Tip chord, ft . . . . .	0.81
Taper ratio . . . . .	0.023
Aspect ratio . . . . .	2.08
Sweep at leading edge, deg . . . . .	60.1
Sweep at trailing edge, deg . . . . .	-5
Incidence, deg . . . . .	0
Dihedral, deg . . . . .	0
Conical camber (leading edge), percent local semispan . . . . .	6.3
Geometric twist, deg . . . . .	0
Inboard fence, percent semispan . . . . .	37
Outboard fence, percent semispan . . . . .	67
Tip reflex, deg . . . . .	6
Maximum thickness:	
Root, percent chord . . . . .	3.9
Outboard edge of elevon, percent chord . . . . .	3.5
Approximate test wing loading, lb/sq ft . . . . .	35

## Elevons:

Area (total, rearward of hinge line), sq ft . . . . .	67.2
Span (one elevon), ft . . . . .	12.89

## Vertical tail:

Airfoil section . . . . .	NACA 0004-65 (Modified)
Area (above waterline 33), sq ft . . . . .	95.1
Aspect ratio . . . . .	1.4
Sweepback of leading edge, deg . . . . .	52.5
Sweepback of trailing edge, deg . . . . .	0

## Fuselage:

Length, ft . . . . .	63.3
Maximum diameter, ft . . . . .	6.5
Total inlet capture area, sq ft . . . . .	4.6
Equivalent-body fineness ratio . . . . .	9.1

## Power plant:

Installed static thrust at sea level, lb . . . . .	8,800
Installed static thrust at sea level (with afterburner), lb . . . . .	13,200

## Test center-of-gravity location, percent mean aerodynamic

chord . . . . .	28 to 29
-----------------	----------

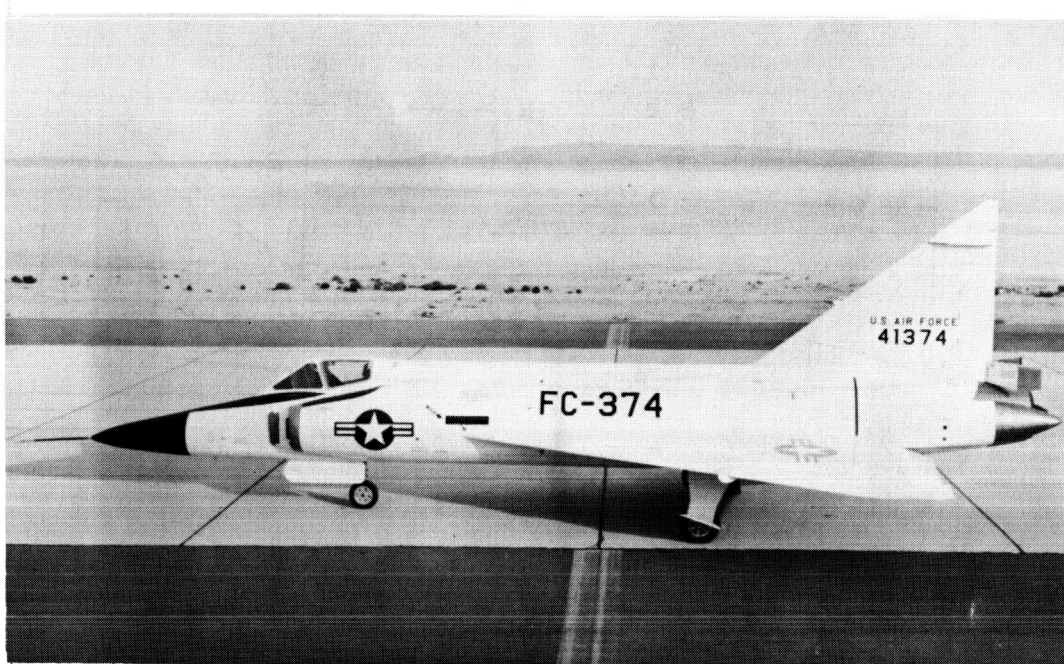
TABLE II.- SUMMARY OF OVERALL DRAG FOR ALL TEST CONDITIONS

Speed range	M $\approx$ 0.8						M $\approx$ 1.1					
Lift range	$C_L \approx 0.050$						$C_L \approx 0.025$					
hp, ft	10,000	15,000	20,000	30,000	35,000	20,000	25,000	30,000	37,000	44,000		
$R_{ft} \times 10^{-6}$	4.3	3.7	3.2	2.3	1.9	4.3	3.7	3.2	2.3	1.7		
R $\times 10^{-6}$ , based on the mean test chord	60.6	52.2	45.1	32.4	26.8	60.6	52.2	45.1	32.4	23.9		
Test-surface finish	Drag coefficient based on wing area, S											
Production with natural transition	0.0104 3	0.0102 5	0.0105 3	0.0094 2	-----	0.0254 3	0.0250 3	0.0239 3	0.0234 1	0.0234 1		
Production with forced transition	0.0107 1	0.0108 1	0.0107 1	-----	-----	0.0256 1	0.0255 1	-----	-----	-----		
Production (weighted mean)	0.0105 4	0.0103 6	0.0106 4	-----	-----	0.0254 4	0.0251 4	-----	-----	-----		
220 grit, of k $\approx$ 0.002 in.	0.0110 1	-----	-----	-----	-----	0.0258 1	0.0255 2	0.0252 1	0.0246 1	-----		
80 grit, of k $\approx$ 0.006 in.	0.0137 1	0.0135 1	0.0134 2	-----	0.0129 1	-----	0.0274 2	-----	-----	-----		

Note: Subscripts indicate number of test runs represented by each value of  $C_D$ .

TABLE III.- COMPARISON OF SKIN DRAG COEFFICIENTS BASED ON FLIGHT MEASUREMENTS  
WITH TERMINAL COEFFICIENTS FOR A SIMILAR ROUGHNESS

M	R $\times 10^{-6}$	80-grit roughness, k $\approx 0.006$ in.			220-grit roughness, k $\approx 0.002$ in.			Production finish
		C <sub>f</sub> (present tests)	C <sub>f</sub> (terminal; ref. 7)	C <sub>f</sub> (terminal; ref. 8)	C <sub>f</sub> (present tests)	C <sub>f</sub> (terminal; ref. 7)	C <sub>f</sub> (terminal; ref. 8)	
0.8	45.1	0.0039	0.00398	0.00373	-----	-----	-----	0.00229
	52.2	.0041	.00398	.00373	-----	-----	-----	.00224
	60.6	.0041	.00398	.00373	0.0025	0.00323	0.00318	.00219
1.1	52.2	.0035	.00398	.00373	.0024	.00323	.00318	.00216
	60.6	-----	-----	-----	.0023	.00323	.00318	.00211



E-3314

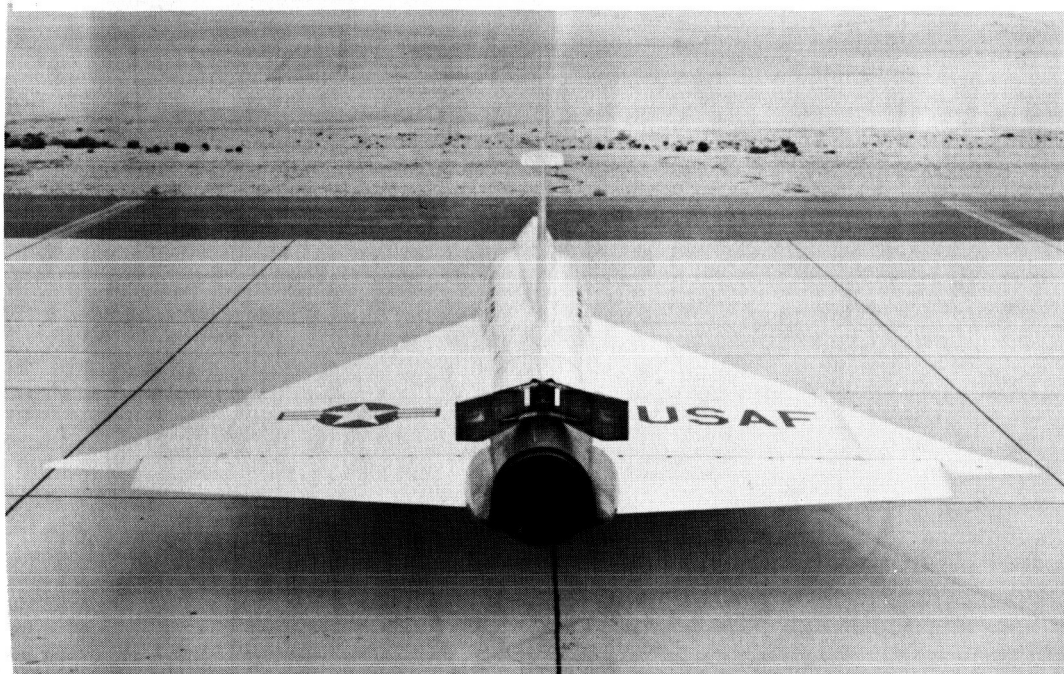


Figure 1.- General photographs of the test airplane. E-3310

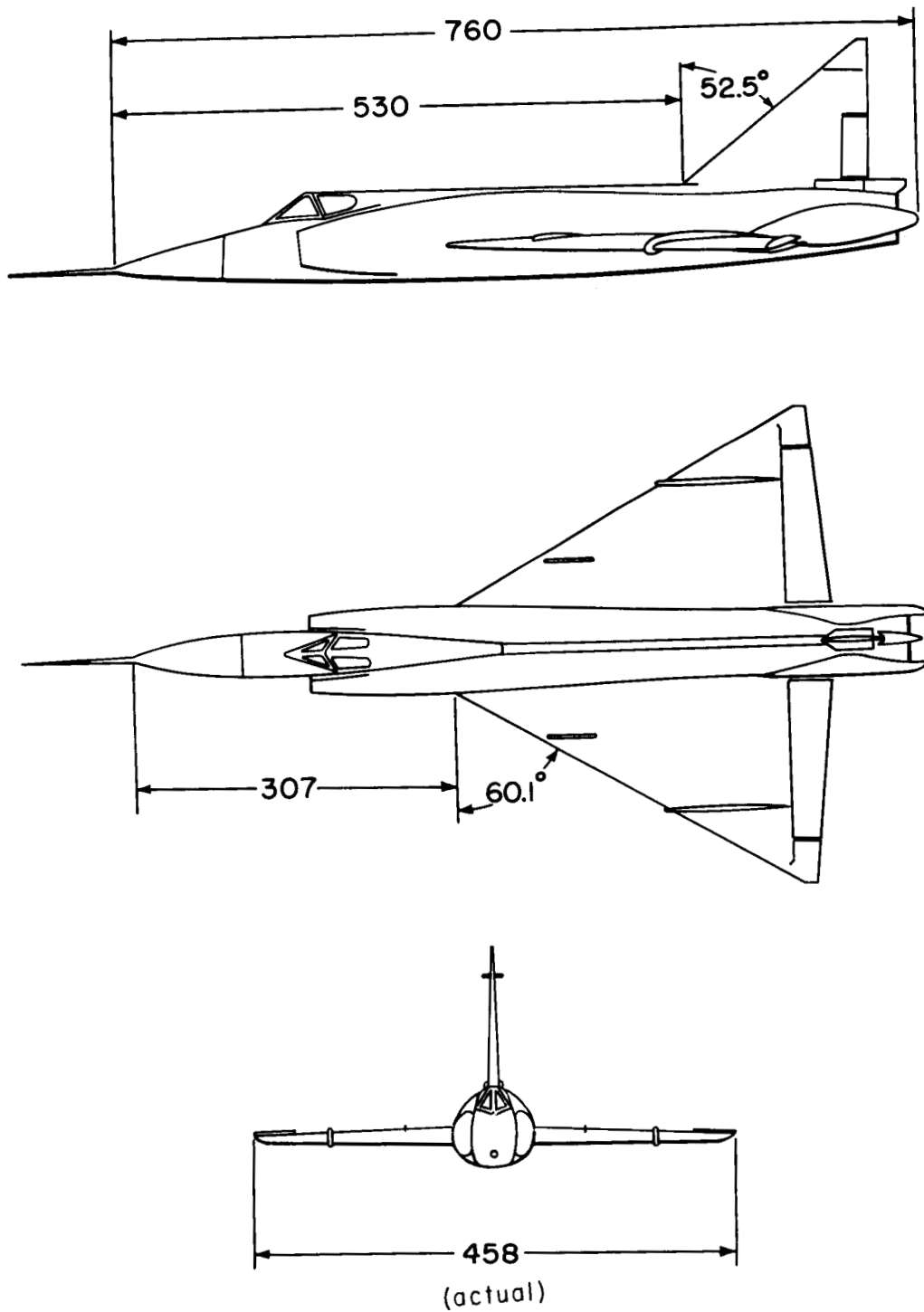


Figure 2.- Three-view drawing of test airplane. All dimensions in inches.

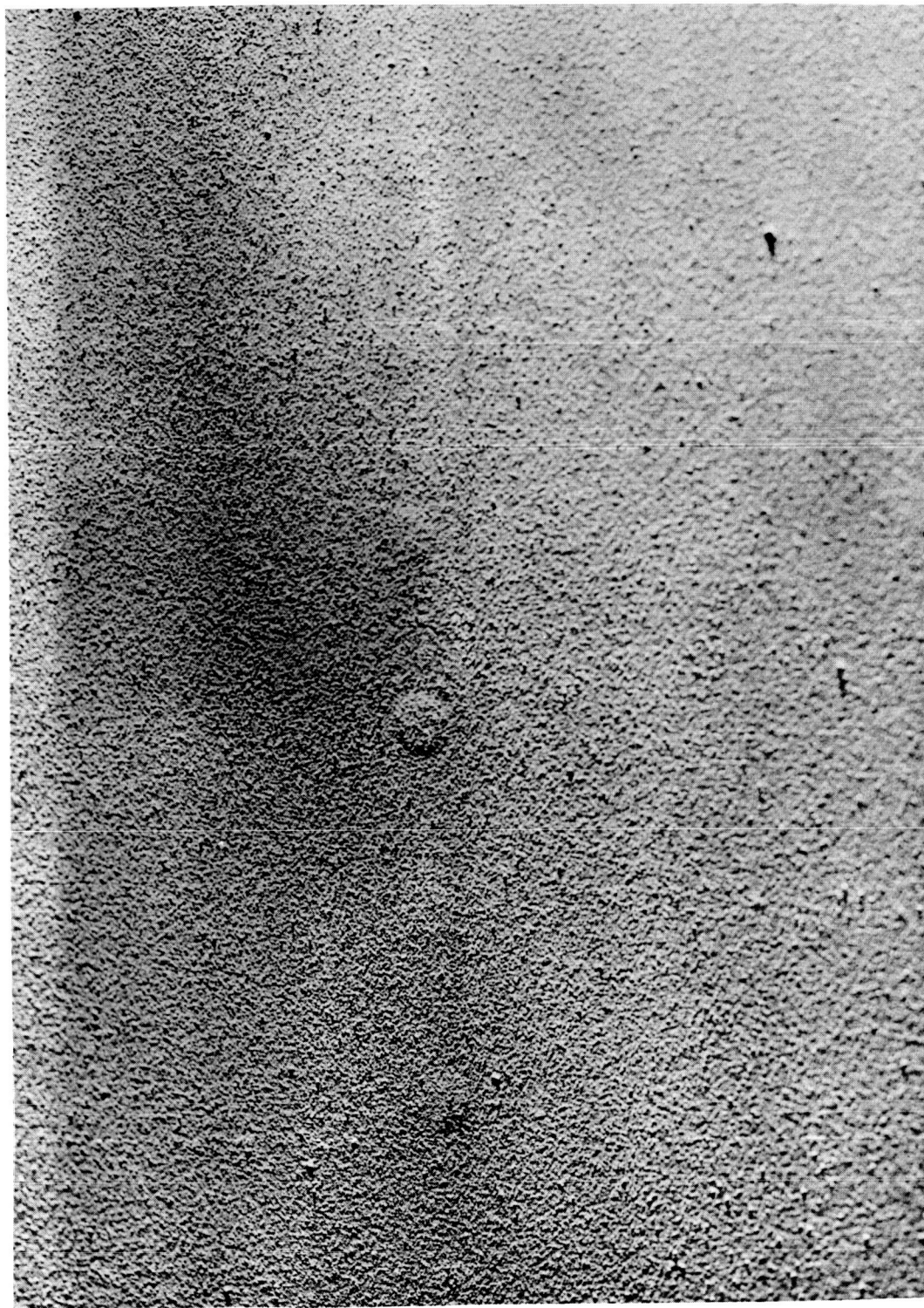


Figure 3.- Photograph of 220-grit surface.

E-3464



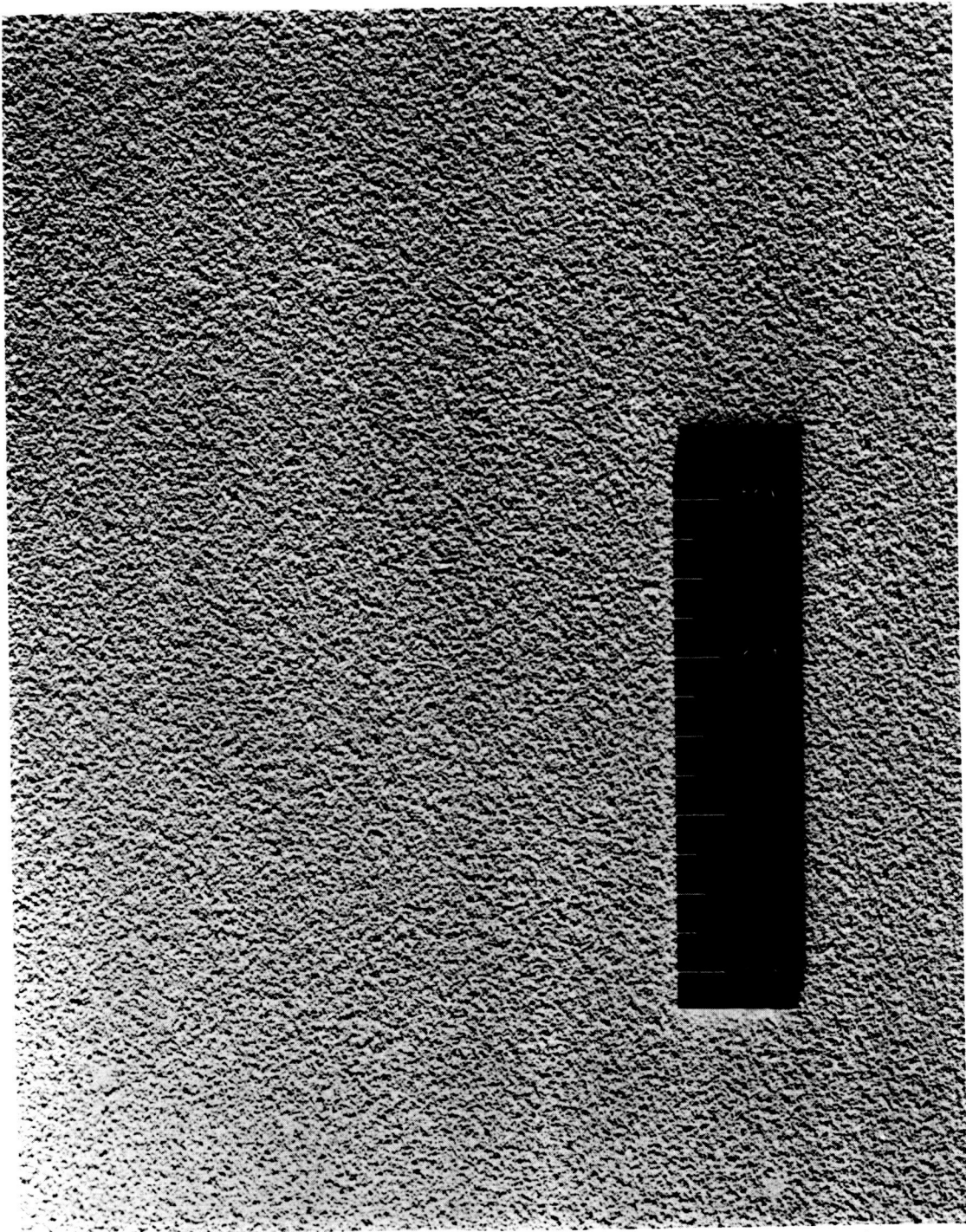


Figure 4.- Photograph of 80-grit surface. E-4311

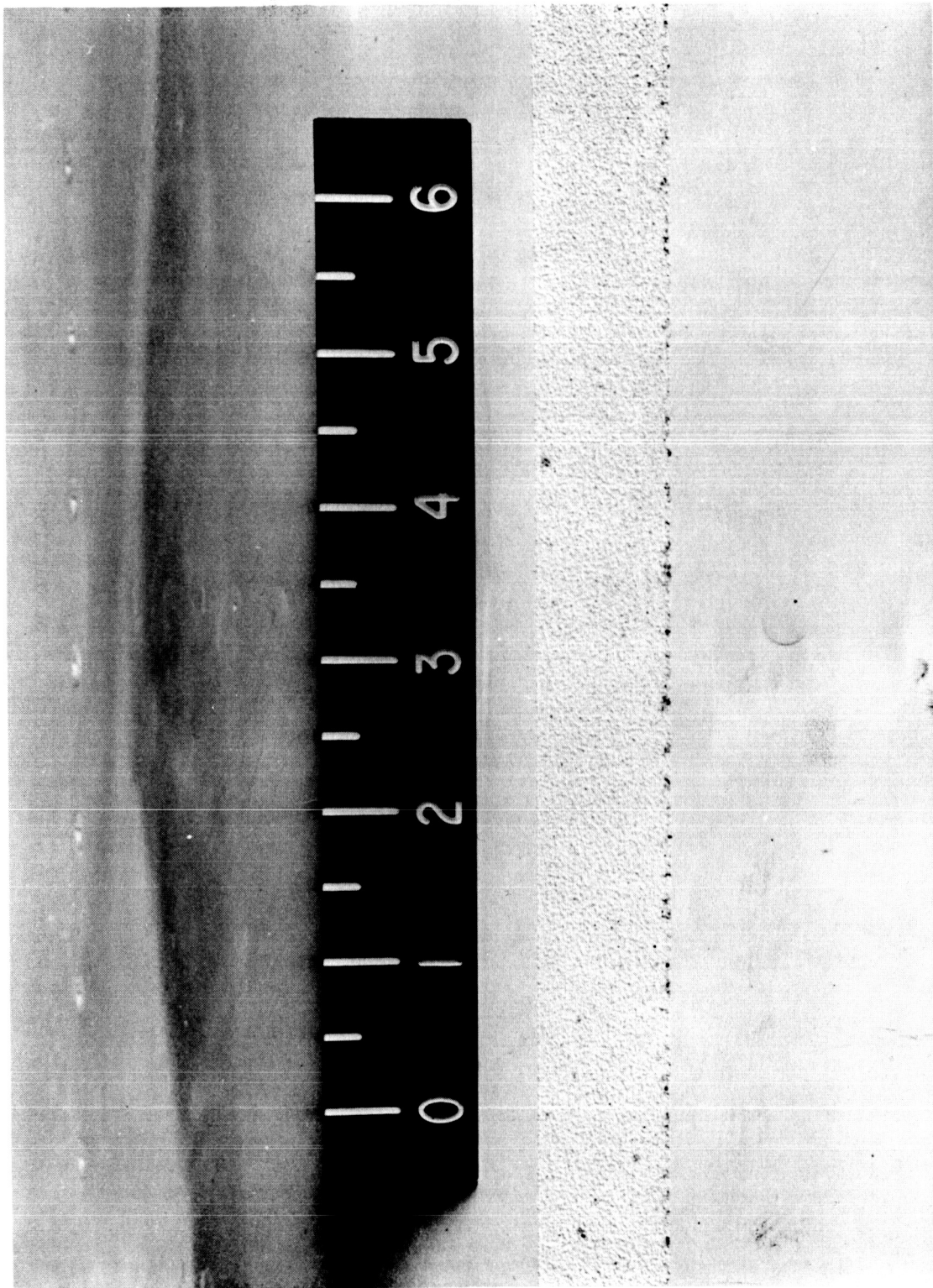


Figure 5.- Photograph of transition strip.

E-4116



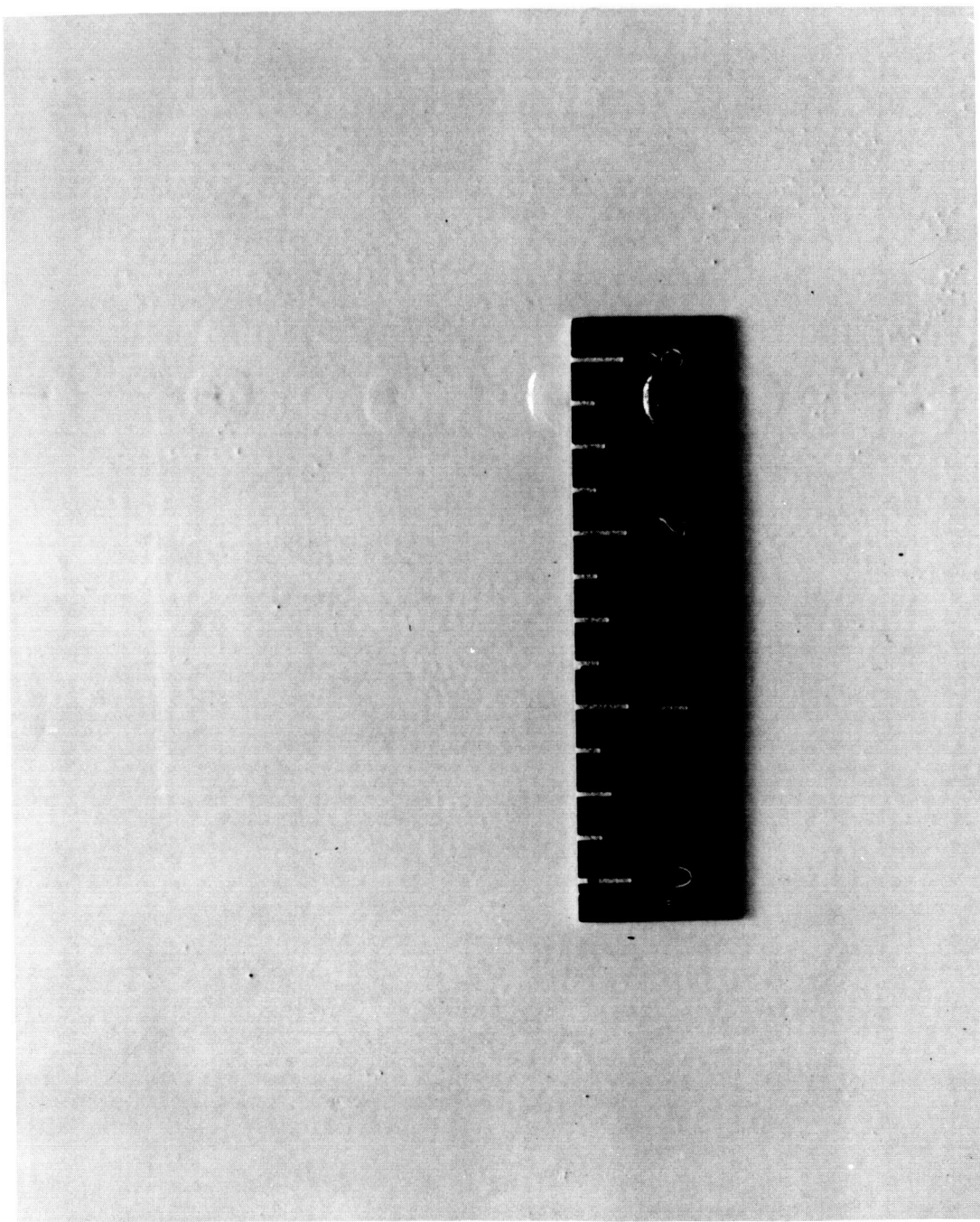


Figure 6.- Photograph of production finish. E-4239

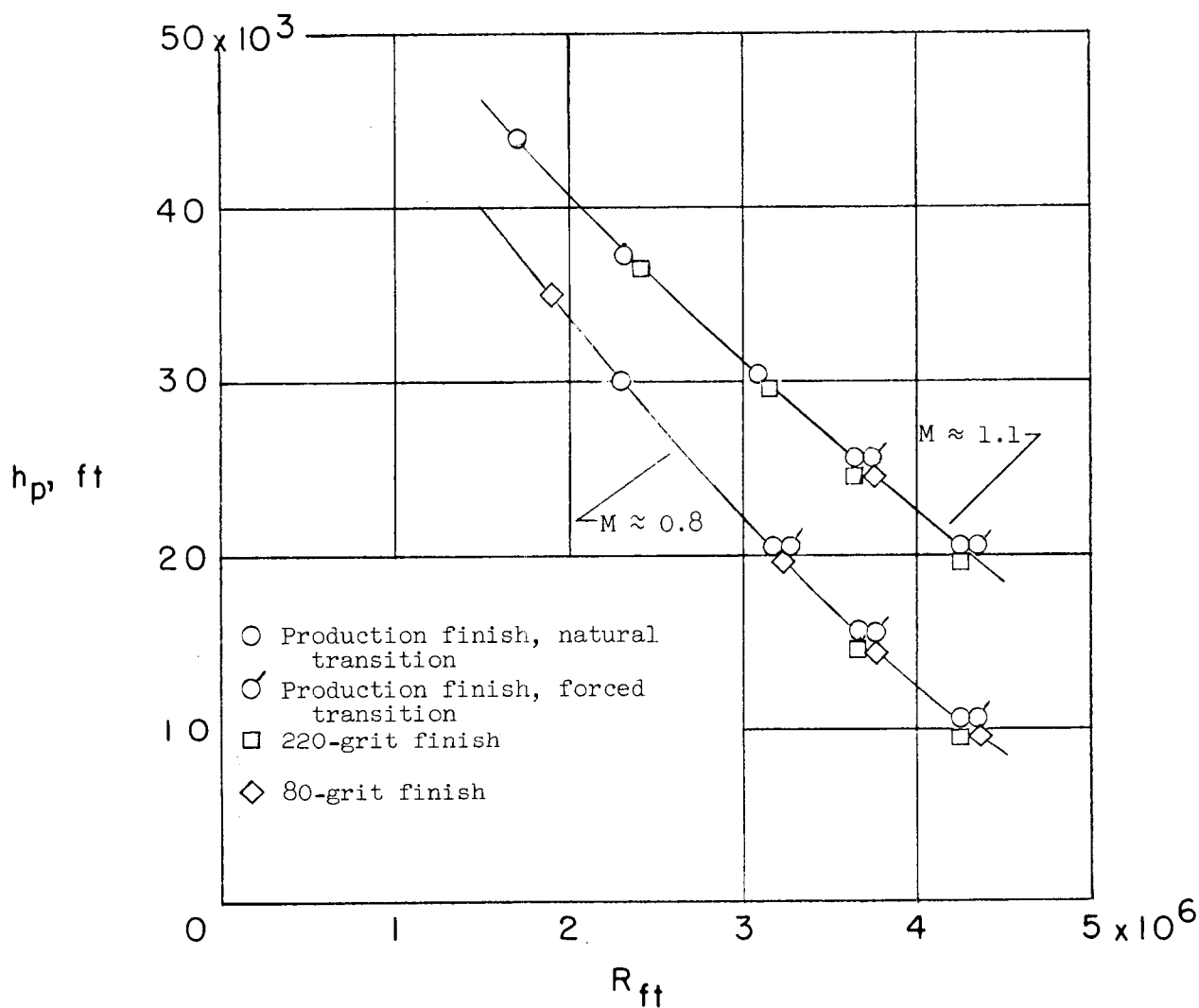


Figure 7.- Summary of test conditions showing approximate values of Reynolds number obtained for the various test surfaces.

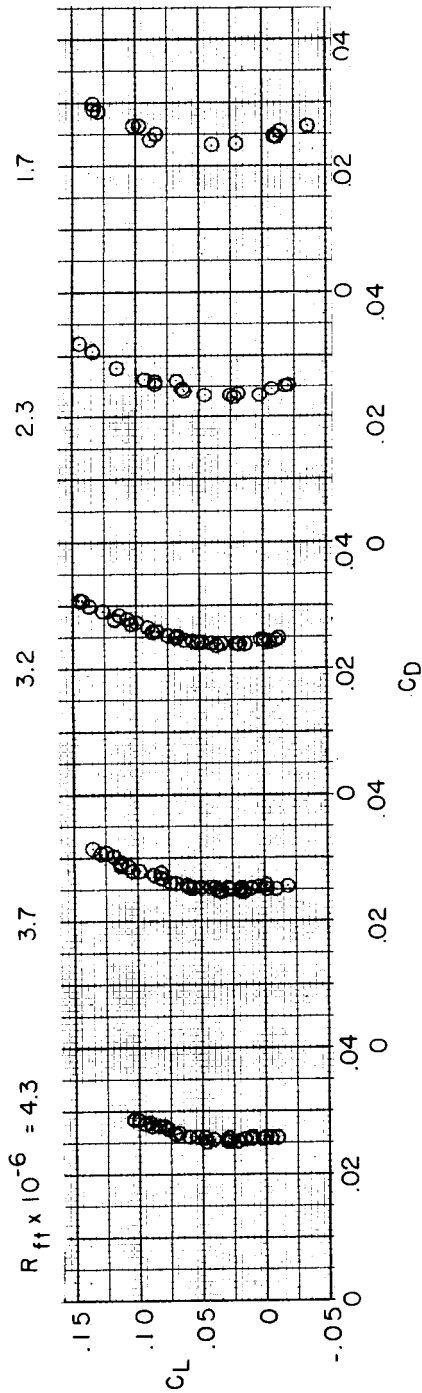
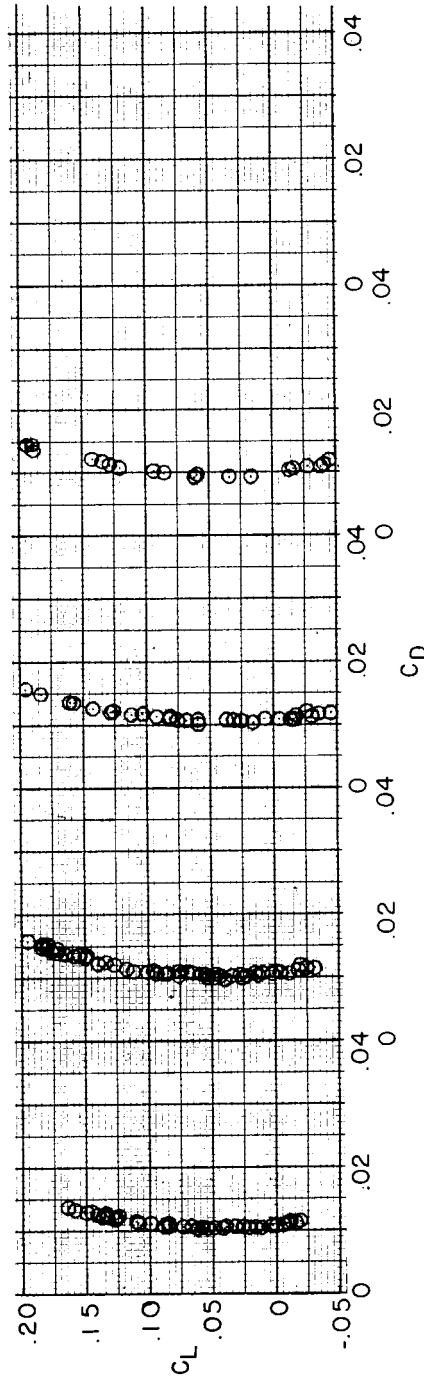
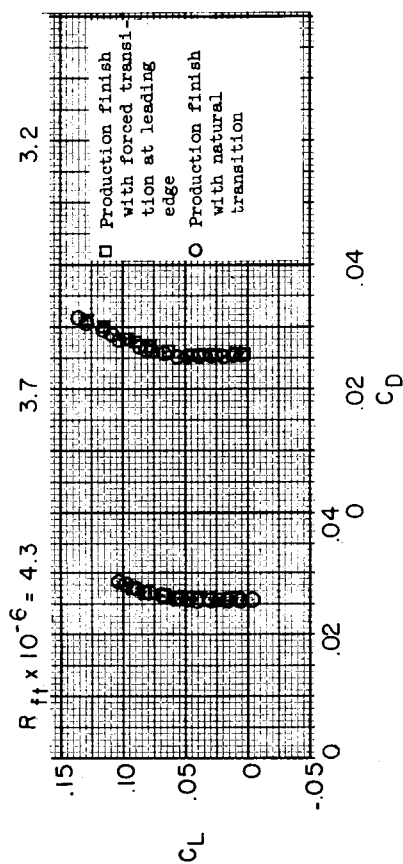
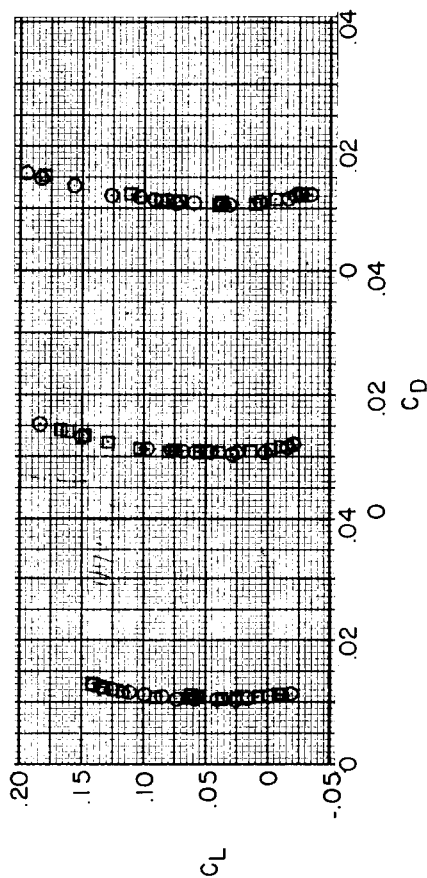
(a)  $M \approx 1.1$ .(b)  $M \approx 0.8$ .

Figure 8.- The variation of drag coefficient with lift coefficient for several Reynolds number values for Mach numbers of 1.1 and 0.8. Production finish with natural transition.



(a)  $M \approx 1.1$ .



(b)  $M \approx 0.8$ .

Figure 9.- The variation of drag coefficient with lift coefficient for several Reynolds number values for Mach numbers of 1.1 and 0.8 for production finish with forced transition at leading edge and for production finish with natural transition.

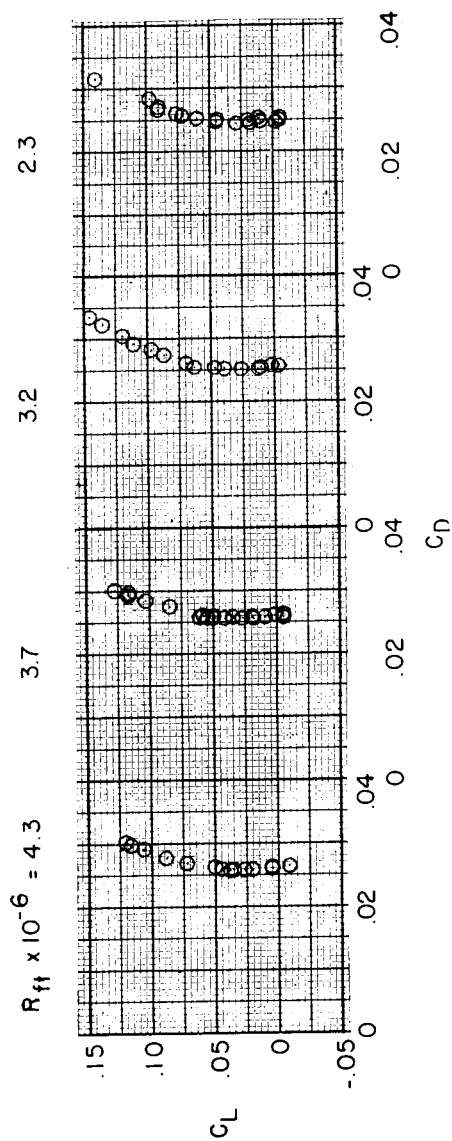
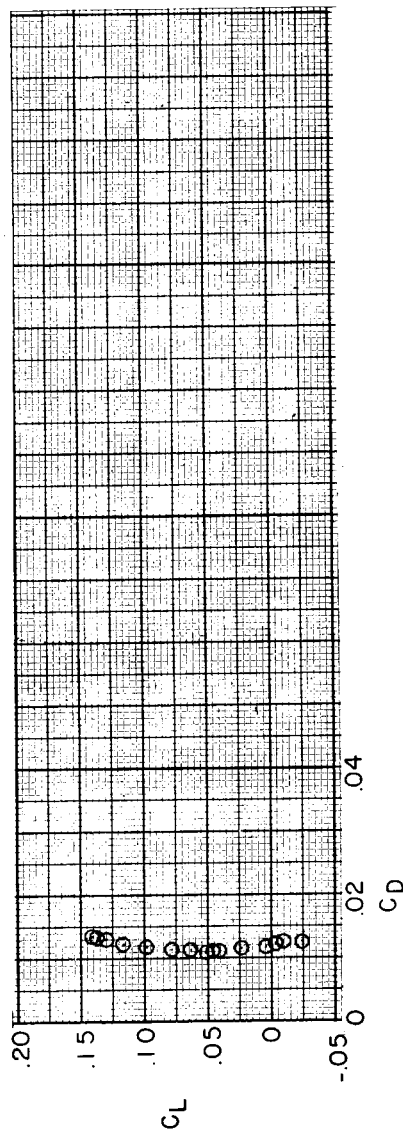
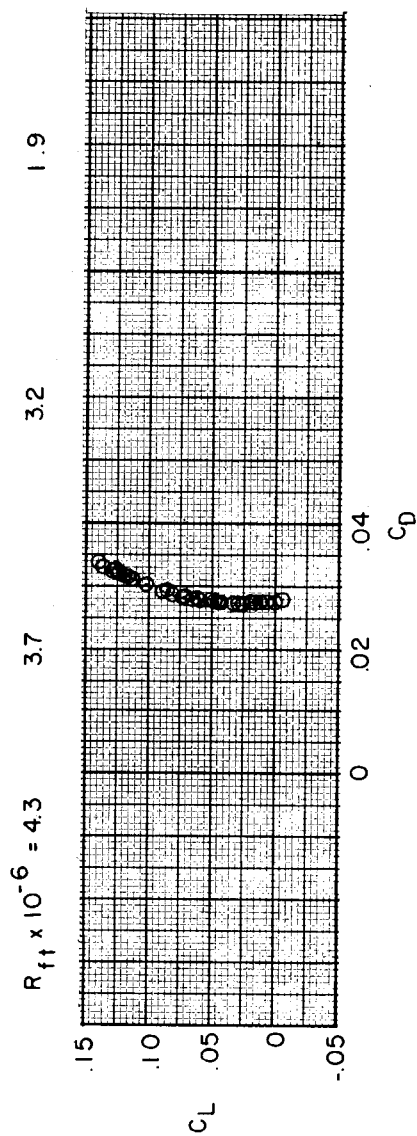
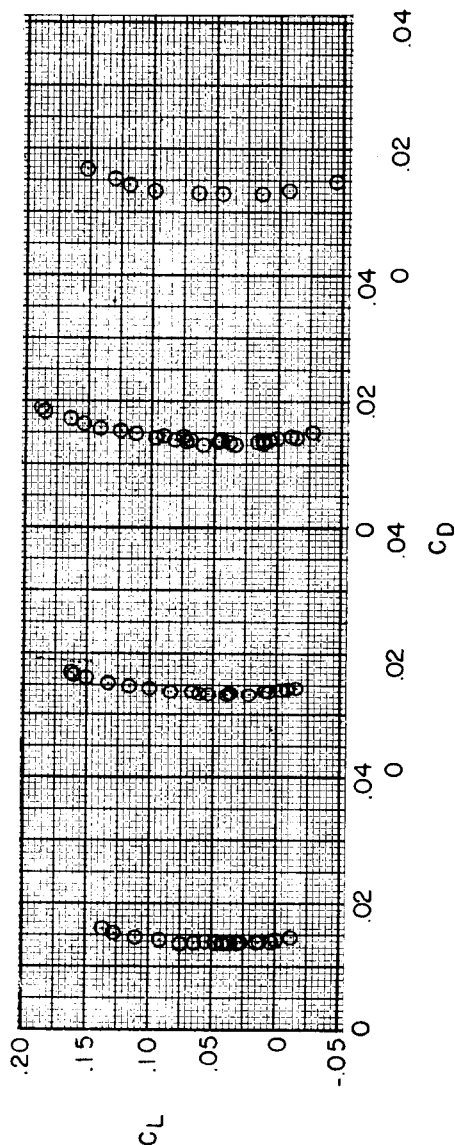
(a)  $M \approx 1.1$ .(b)  $M \approx 0.8$ .

Figure 10.- The variation of drag coefficient with lift coefficient for several Reynolds number values at Mach numbers of 1.1 and 0.8 with 220-grit finish.



(a)  $M \approx 1.1$ .



(b)  $M \approx 0.8$ .

Figure 11.- The variation of drag coefficient with lift coefficient at several Reynolds number values for Mach numbers of 1.1 and 0.8 with 80-grit finish.

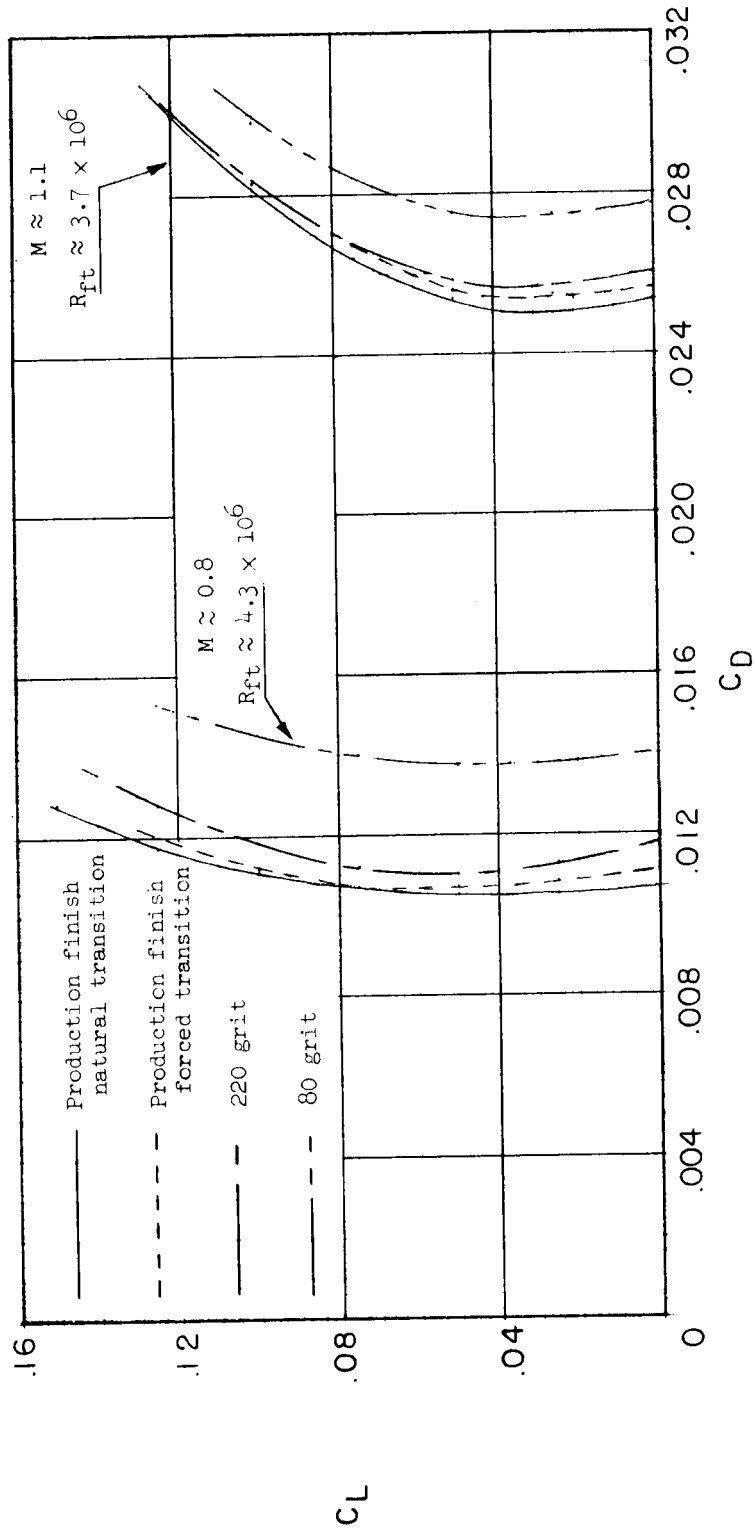


Figure 12.- The variation of drag coefficient with lift coefficient for all test conditions.

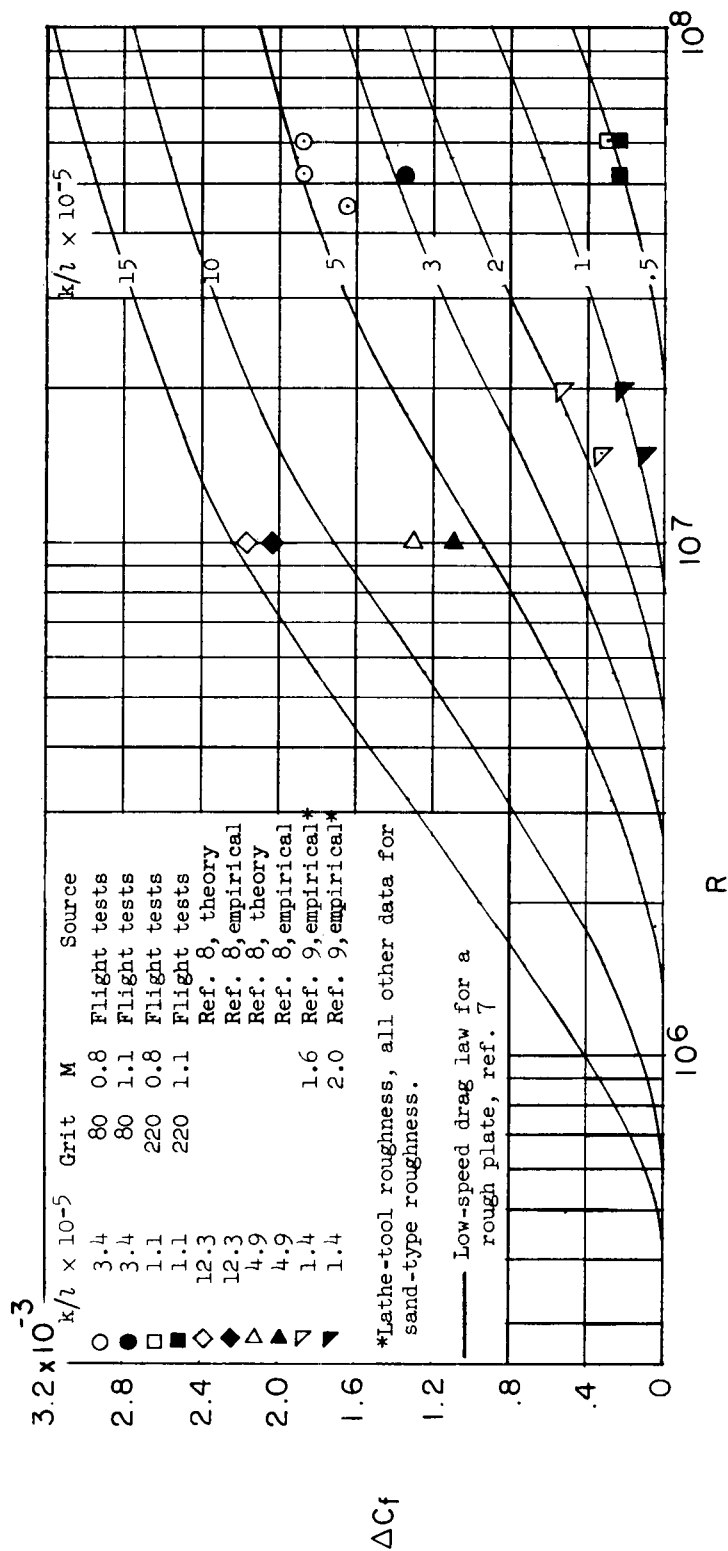


Figure 13.- Comparison of the increase in skin drag coefficient for the present tests with the increase predicted by the low-speed drag law for a rough plate and other empirical results.